JOURNAL OF OPTOELECTRONICS AND ADVANCED MATERIALS, Vol. 11, No. 5, May 2009, p. 648 - 654

Energy relaxation mechanisms and mobility of electrons in n-type InN

MEHMET ARI[a*], HULYA METIN[b]
[a]*University of Erciyes, Department of Physics, Kayseri, Turkey*
[b]*University of Mersin, Department of Physics, Mersin, Turkey*

We present a theoretical model regarding the electron-phonon interactions in n-type InN at a lattice temperature of 1.5 K. A perturbation-based model with a drifted Maxwellian distribution is used for obtaining the energy loss rates and mobility from electron-phonon scattering mechanisms as a function of electron temperature and electron concentration at electron temperature range of 1.5-500 K. We show the importance of acoustic phonon emission due to piezoelectric coupling and deformation potential scattering for energy relaxation processes at low temperature region, T_e<130 K. Above this electron temperature, the polar optic phonon emission dominates the scattering mechanism and causes the reduction of electron mobility. Two transition region were seen between piezoelectric acoustic phonon and deformation potential acoustic phonon at about T_e=35 K; and between the deformation potential acoustic phonon and polar optic phonon at T_e =130 K. The model calculation results have been compared with available experimental results and a good agreement has been obtained for the energy loss rates and mobility of electrons. Also, the polar optic phonon scattering time has been obtained about 23 fs.

(Received April 28, 2009; accepted May 25, 2009)

Keywords: Electron-Phonon Interaction; Electron Temperature; Mobility; InN

1. Introduction

Nitride based materials are most promising materials for high temperature, high frequency and radiation hard applications. These materials are in forefront of the semiconductor research. Nitride based materials such as GaN, AlN an InN have been intensively applied in optoelectronic and electronic device technology [1-9]. This kind of optoelectronic devices are required for solid state lighting, color display, laser printers, high density information storage etc. Also, blue light emitting diodes have been constracted and much current work is aimed at realising practical laser diodes from InN/GaN or AlN/GaN based semiconductor materials [10]. The nitrides are also attractive for use in field effect transistors intended to operate at high power and temperature.

In contrast to GaN and AlN, very little is known about InN. Recently, InN has been proved to be narrow band gap materials with energy band gap of about 0.7 eV at low temperature and 0.65 eV at room temperature [11-14]. This observation has an enormous impact on III-nitride based research. This also makes the nitrides much more attractive than before for optoelectronic device applications. Due to the narrow band gap of InN, it is possible to fabricate the infrared emission of diode. The potential of extending the band gap energies of the group III-nitride in to the near infrared spectral region has generated considerable interest, and extensive research efforts have been initiated by researchers. Furthermore, solar cells with high efficiency can be also made on nitride based alloys which cover the range of 0.65-6.2 eV.

Investigation of electron dynamics in semiconductors has played a central role in III-V materials including nitrides. In order to analyse and improve the performances of devices based on these materials, an understanding of carriers transport is necessary. The energy loss mechanisms provide important information about electron-phonon scattering and give valuable knowledge for through understanding of nitride based materials semiconductor devices. A detailed study of the energy loss processes and mobility with the determination of the dominant scattering mechanisms in these materials is crucial for obtaining a comprehensive understanding of the carrier dynamics. For these reasons, the energy relaxation mechanisms and the scattering processes have been extensively studied in III-V material based devices [15-25].

The main objective of this work is to investigate the energy relaxation mechanisms of electrons in n-type InN. We have performed analytical electron temperature based model by using a weak perturbation based method in order to investigate electron temperature and electron concentration dependence of energy loss rates and mobility at lattice temperature T_o=1.5 K. A detailed description of main scattering mechanisms responsible for the energy relaxation processes and mobility has been determined at electron temperature of 1.5-500 K. The model calculations have been carried out by using the theoretical approach given by Shah [23], Conwell [24], Seeger [25]. The model has been modified in order to include the dependence on electron concentration. This allows us to determine the electron temperature dependence of mobility and the energy loss rates of InN for different electron concentrations.

2. Theoretical background

In order to investigate the contribution of energy dissipation of electrons via phonon scattering, the energy relaxation rates have to be determined. Theoretically calculated energy loss rates differ from each other

depending on the theoretical models adopted in their calculations. In order to test various theoretical predictions about the behaviour of energy loss processes of the carriers due to different type of scattering mechanisms, one has to know which type of scattering is predominant in a given sample of material, temperature, carrier concentration and electric field range. In the materials of interest, the interaction of electrons and phonons may be treated by perturbation theory.

In view of the importance of InN, electronic properties of the materials need a through investigation for application in high frequency and high performance areas. Several authors have already undertaken transport studies of the carriers both at low and high temperature [26-31]. Scattering of electrons by phonons and other electrons play a central role in transport process. The scattering mechanisms that affect the energy loss processes and limit the mobility of the carriers are mainly acoustic phonons due to PZ coupling and DP interaction and also inelastic PO phonons. The electron-electron (e-e) interactions conserve the energy inside the electronic system and have no direct effect on the electron energy dissipation. However, these interactions can influence the energy balance indirectly. When the energy loss is enhanced during an e-e collision, one of the colliding electrons acquires enough energy for emission of phonons while none of the colliding electrons has had enough energy before the collision.

The electron-phonon scattering rate and their dependence of electron temperature and electric field can be used in order to determine the energy loss of an electronic system which gains energy from electric field and should transfer this energy to the lattice through collisions. As a results, the average energy on the electron temperature of the electrons increases with the consequent decrease in the momentum relaxation time. Under steady state conditions, warm and hot electron phenomena are governed by the balance between the power input to the electronic system from the applied electric field and the energy loss of electrons, which are usually dominated by the inelastic collisions between the electrons and the phonons. It is possible that the fraction of excess energy leading to the heating of electrons can be known by using the power supply to the electronic system. The joule input power per electron should to be equated to the energy loss rate of electrons. So, the energy loss of electrons can be taken equal to the energy loss rate of phonons. By using balance equations, the energy loss rates and mobility of electrons as a function of electron temperature and electron concentration can be determined and the applied field dependence of electron temperature and drift velocity can be obtained.

2.1. Energy loss rates

The model calculations for the steady state energy loss rates are based on the fundamental assumption that the (e-e) scattering results in the thermalisation of the electrons. Hence, a non-equilibrium electron gas can be presented by a statistical electron temperature, T_e. In order to obtain the average rate of energy loss for electrons, it is necessary to specify the distribution function. A distribution that has been found convenient to use in this connection is the drifted Maxwell-Boltzmann distribution for the non-degenerate case. A method of calculating the electron temperature dependence of energy loss of electrons with simplifying of a Maxwell-Boltzmann distribution with an electron temperature T_e consist of averaging momentum relaxation time over this distribution and calculating the energy loss rates as a function of electron temperature, T_e, from momentum and energy balance equations. The validity of this distribution, which depends on the dominance of the e–e scattering on the other scattering mechanism in thermalizing the electron distribution, is expected to hold even at high field due to the high electron concentration. Thus, we assume that the distribution function of the central valley electrons to be a drifted Maxwell-Boltzmann distribution.

In the electron temperature approach, the expression for the energy loss rate term, $\langle d\varepsilon/dt \rangle$, as a function of electron temperature T_e and electron concentration n_e, can be defined by considering the different scattering processes. We expect that the energy flow from the electronic system will be mainly through the acoustic phonon emission via the (DP) and the (PZ) coupling which dominant mechanisms of energy loss at low and intermediate temperature value. At high temperatures, the dominant scattering mechanism is the (PO) phonon scattering mechanism. Therefore, the main scattering mechanisms are the PZ acoustic phonon, the DP acoustic phonon and the PO phonon in n-type InN.

If a crystal consists of dissimilar atoms such as InN, the bonds are partly ionic and the unit cell does not contain a centre of symmetry and exhibiting piezoelectric effects, especially at very low temperature, electron may be scattered by the acoustic phonons due to the PZ coupling. To obtain the energy relaxation rates of electrons, $\langle d\varepsilon/dt \rangle$, momentum and energy balance equations can be used. For the calculation of the energy loss rate as a function of electron temperature and electron concentration due to acoustic phonon via the PZ scattering for the non-degenerate case, can be given by [23-25],

$$\left\langle \frac{d\varepsilon}{dt} \right\rangle_{pz} = \frac{1}{n_e}\left(\frac{0.8m^3(e_{14}ek_BT_e)^2}{\pi^3\hbar^5\rho(\varepsilon_o\varepsilon_s)^2} \right)\left(1-\frac{T_o}{T_e}\right)F_o(\eta) \quad (1)$$

here, k_B is the Boltzmann constant, ρ is the density of InN, e is the electric charge of electron, m is the effective mass of electron, T_o is the lattice temperature, u_l is the longitudinal sound velocity, n_e is the electron concentration, e_{14} is piezoelectric constant, ε_s is the static dielectric constant of InN, ε_o is the free space dielectric constant, η is the reduced fermi energy and $F_j(\eta)$ are fermi integrals.

The scattering of conduction electrons by acoustic phonons also requires the theorem of the deformation potential. The acoustic phonon mode scattering mechanism is that due to the DP interaction is effective at low and intermediate temperatures. In steady state, when all the acoustic modes are fully excited, the average energy loss per unit time of an electron to the crystal lattice due to acoustic phonon emission via the DP interaction at temperature T_e, is given by,

$$\left\langle \frac{d\varepsilon}{dt} \right\rangle_{dp} = \frac{1}{n_e}\left(\frac{8D^2 (k_B T_e)^3 m^4}{\pi^3 \hbar^7 \rho} \right)\left(1 - \frac{T_o}{T_e}\right) F_1(\eta) \qquad (2)$$

where D is the deformation potential constant.

At high electron temperatures, the interaction of electrons with the optic phonons is known as the polar optic phonon scattering which becomes to dominate the energy relaxation mechanism. In the absence of hot phonon effects as assuming $T_e >> T_o$, the average energy loss rate per electron energy due to the PO phonon emissions is given by the expression,

$$\left\langle \frac{d\varepsilon}{dt} \right\rangle_{po} = \frac{1}{n_e}\left(\frac{(\hbar\omega_o k_B T_e)^{3/2} (em)^2}{4\pi^3 \hbar^5 \varepsilon_o} \right)\left(\frac{1}{\varepsilon_\infty} - \frac{1}{\varepsilon_s} \right) \left(\frac{e^{X_o - X_e} - 1}{e^{X_o} - 1} X_e^{1/2} e^{X_e/2} \right) K_o\left(\frac{X_e}{2} \right) F_{1/2}(\eta) \qquad (3)$$

here, $X_e = \hbar\omega_o / k_B T_e$, $X_o = \hbar\omega_o / k_B T_o$, ω_o is the optical phonon frequency for InN. K_o and K_1 are the Modified Bessel Functions of the second kind. ε_∞ is the high frequency dielectric constant of InN.

2.2. Mobility

The total mobility can be calculated by considering different energy loss mechanisms. The expressions for various mobility, μ_j can be given by

$$\sum_i \left\langle \frac{d\varepsilon}{dt} \right\rangle_i = e E^2 (\sum_j \mu_j) \qquad (4)$$

and the scattering limited total mobility μ by using Matthiessen's rule, can be written as,

$$\frac{1}{\mu} = \sum_j \frac{1}{\mu_j} \qquad (5)$$

The scattering of electron by acoustic phonon emission is found to be the dominant mechanism at low electron temperatures. The mobility determined by the scattering of electrons due to piezoelectric coupled acoustic phonon emission can be given by,

$$\mu_{pz} = \frac{1}{n_e}\left(\frac{8\rho k_B T_e^2}{1.2\pi e \hbar T_o} \right)\left(\frac{u_l \varepsilon_o \varepsilon_s}{e_{14}} \right)^2 F_{1/2}(\eta) \qquad (6)$$

The mobility of electrons determined by the acoustic phonon due to deformation potential can be written,

$$\mu_{dp} = \frac{1}{n_e}\left(\frac{4 e \rho u_l^2 T_e}{3\pi D^2 m \hbar T_o} \right) F_1(\eta) \qquad (7)$$

At high temperatures, electrons lose their energies by emitting longitudinal optic phonon. Hence, the dominant scattering mechanism is the PO phonon scattering mechanism. The mobility limited by polar optic phonon can be given by,

$$\mu_{po} = \frac{1}{n_e}\left(\frac{3m(k_B T_e)^3}{2^{5/2}\pi E_o \hbar^4 \omega_o} \right)\left(\frac{e^{X_o} - 1}{e^{X_e/2}} \right) \left[\left(e^{X_o - X_e} + 1\right) K_1(X_e/2) + \left(e^{X_o - X_e} - 1\right) K_o(X_e/2) \right]^{-1} F_{1/2}(\eta) \qquad (8)$$

here E_o is the critical electric field strength. The theoretical results were obtained by numerical evaluation of equations (1-8). The values of the parameters used in the calculations are given in Table 1 [26-28].

Table 1 Values of InN materials constant used in the calculations [26-28]

Electron effective mass (m_o)	m=0.11
High frequency dielectric constant (ε_o)	ε_∞=8.4
Static dielectric constant (ε_o)	ε_s=15.3
LO-optic phonon energy (meV)	$\hbar\omega_o$ = 73
Longitudinal acoustic phonon velocity (m/s)	u_l=5.24x10^3
Piezoelectric constant (Cm^{-2})	e_{14}=0.375
Deformation Potential Constant (eV)	D=7.1
Mass density (g/cm^3)	ρ=6.81

3. Results and discussion

Fig. 1 shows the theoretical results of the energy loss rates per electron as a function of electron temperature in the range of 1.5-500 K. The calculations were carried out for an electron concentration of 9x10^{24} m^{-3}. Considering the low and intermediate electron temperature region, the lines through the experimental values in Fig.1 are obtained by numerical evaluation of eqs. (1-3). The calculated results confirm that the acoustic phonon scattering due to the PZ and DP interaction are dominant on the energy loss process in the electron temperature range of T_e<130 K. At very low electron temperatures T_e<35 K, the energy loss per electron is mainly due to acoustic phonon emission via unscreened PZ coupling which is clearly seen from Fig. 1. Above this electron temperature, the deformation potential acoustic phonon emission starts to influence the energy loss process and a crossover from the PZ acoustic phonon emission to the DP acoustic phonon emission occurs

corresponding to T_e=35 K. This transition region can be clearly from Fig. 1. The acoustic phonon scattering due to deformation potential stays effective up to electron temperature reaches to 130 K. Fig. 1 also shows that, above an electron temperature of 130 K, energy loss of electrons is mainly due to polar optic phonon emission. Therefore, another crossover exists from energy loss of electron due to deformation potential acoustic phonon emission to energy loss via polar optic phonon emission at electron temperature 130 K which corresponds to the energy loss value of about $4x10^{-11}$ W per electron.

In Fig. 2, we have plotted the energy loss rates per electron versus inverse of electron temperatures for electron concentration as the same of Fig. 1. Fig. 2 shows that the energy loss per electron is seen to increase with increasing T_e. It is also clear from Fig. 2 that the acoustic phonon mode scattering due to the PZ and DP coupling are determine the energy loss processes in the electron temperature range of $1.5<T_e<130$ K, where can be called the acoustic phonon region. In addition, a very good agreement has been obtained between experimental and calculated results for electron temperatures above about 130 K, which can be called optical phonon emission regime. The optic phonon scattering time constant of InN can be obtained by a plot of $\ln(P_e)$ versus inverse of electron temperature ($1/T_e$) gives straight line at high electron temperatures, which can be seen from Fig. 2. The line intercepts the power axis at $\langle d\varepsilon/dt\rangle = \hbar\omega_o/\tau$ which is equal to 1.6×10^{-6} W per electron, from this was determined the optic phonon scattering time τ of 23.3 fs. We compared the theoretical results of energy loss rates with the experimental results [29, 30]. It can be seen from Fig. 1 and Fig. 2 that a good agreement is observed between the theoretical and experimental results. Therefore, we can conclude that the theoretical model works well and it is well able to account for the important features of energy loss mechanisms of InN structure at both low and high electron temperature ranges.

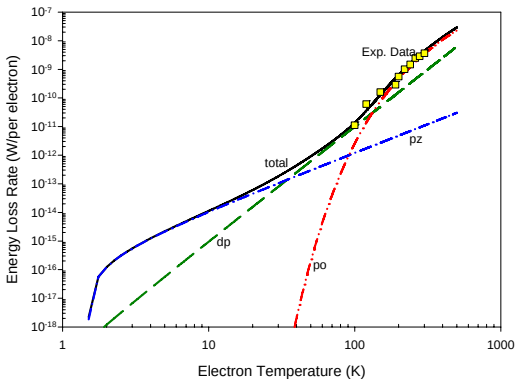

Fig. 1. The energy loss rates of electrons as a function of electron temperature in InN for the electron concentration of 9.0 $\times10^{24}$ m^{-3} at lattice temperature T_o=1.5 K. The contributions of piezoelectric coupling (dash-dot line (pz)), deformation potential (dash line (dp)) and polar optic phonon emission (dash-dot-dot line (po)) are shown by lines. The solid line shows the total contribution of the whole scattering mechanisms. The squares show the experimental results of Zanato et al [29].

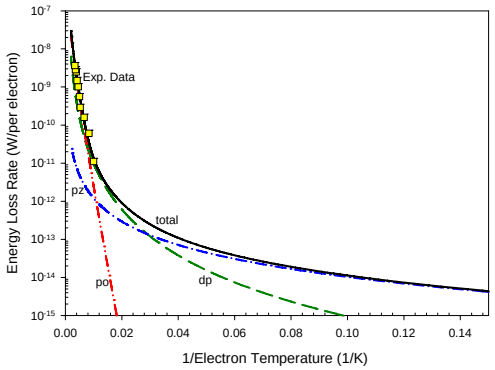

Fig.2. The theoretical results for power loss per electron, P_e as a function of inverse electron temperature, $1/T_e$ (lines) for $n_e=9.0x10^{24}$ m^{-3}. The experimental results of Zanato et al [29] are also shown as squares.

To test the validity of the theoretical model over an electron temperature range, we also calculate the mobility of electrons for different electron concentrations. The expressions which are used in this work, for the various energy loss rates and mobility terms are also depend on electron concentration. This gives us to calculate the mobility and the energy loss rates as a function of electron concentration. Fig. 3 shows the electron temperature dependence of theoretically calculated mobility results for electron concentration of $1.8x10^{23}$ m^{-3}. The calculated results of mobility were compared with experimental mobility measurement of Tansley et al [31] for three different electron concentrations and shown in Fig. 4. As can be seen in Fig. 3 and Fig. 4 that, at low electron temperature range (T_e<130 K), the mobility increases with increasing electron temperature, where the acoustic mode scattering dominates the transport process. The agreement between the computed results and the available experimental results is good within the experimental uncertainty, especially in the electron temperature range of T_e<130 K.

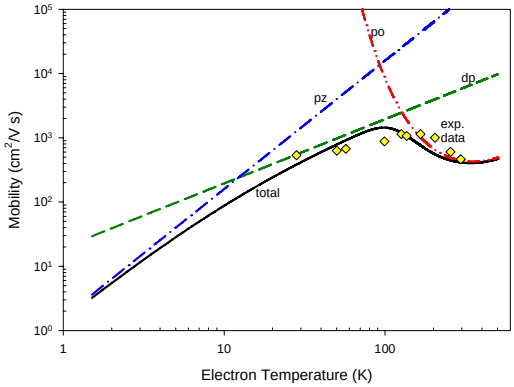

Fig. 3. Electron temperature dependence of electron mobility for the electron concentration of $n_e=1.8x10^{23}m^{-3}$. The lines are the theoretical results and the squares show the experimental results of Tansley et al [31].

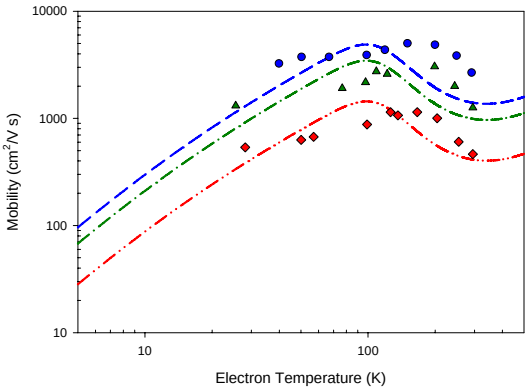

Fig. 4. Mobility of InN versus electron temperature for three different electron concentrations. The lines show the results of theoretical calculations, the dash line is for n_e=5.3×10^{22} m^{-3}, dash-dot line is for n_e=7.5×10^{22} m^{-3} and dash-dot-dot line is for n_e=1.8×10^{23} m^{-3}. The symbols show the experimental results of Tansley et al [31] for the same electron concentrations, circles for n_e=5.3×10^{22}m^{-3}, triangles for n_e = 7.5 × 10^{22} m^{-3} and diamonds for n_e=1.8×10^{23} m^{-3}.

At T_e>130 K, there is a region close to the acoustic-optic phonon crossover where the theoretical results of mobility deviate from the experimental mobility values. This implies that, there are other scattering mechanisms not included to the model that affect the mobility of electrons. There could be several possible reasons for this discrepancy. The samples which are used in the study of Tansley et al [31], might have the strong defect scattering and the momentum conservation selection rule relaxed. Also, the emission of coupled plasmon-optic phonon modes and emission of transverse optic phonons exist in the energy loss processes. The model does not take into account the population of higher subbands which is more likely to occur in InN and also ignores the possible surface charge effect on the electron transport. Another possible scattering mechanism is the intervalley scattering that is also important at high temperature for bulk semiconductors, which is also not included to the theory. In addition, the behaviour of theoretically obtained results are gradually reduced with compared experimental ones, would be expected if there were hot phonons present at this electron temperature region. The results of the hot phonon process are an overall decrease in the drift velocity on effect that has been already revealed in InN [29]. The hot phonon reabsorption not only enhances the momentum relaxation rate but also reduces the energy loss rates. If this is correct, the magnitude of the experimental results should deviate from the theoretical results of the energy loss rate which does not include the hot phonon effect.

We have also obtained electric field and electron temperature dependence of drift velocity by using the equation of $\langle d\varepsilon/dt\rangle = eE\upsilon_d$ for the electron concentration of n_e=9.0×10^{24} m^{-3}. Here, υ_d is the drift velocity and E is the electric field. The drift velocity versus electric field was then calculated. It is clear from Fig. 5 that, the drift velocity is increasing very sharply with electric field in the range of E<200 V/cm, where the acoustic phonon scattering influences the energy loss process. It also shows that, when E >200 V/cm, the drift velocity starts to saturate at about 2.0×10^6 cm/s, corresponds to the electric field region where the optic phonon scattering dominates both the momentum and the energy dissipation. The electric field dependence of the drift velocity also shows that the drift velocity stay almost constant with electric field (up to 1.4x10^4 V/cm) in the same phonon regime. At about T_e≈100 K, the drift velocity reaches the maximum values of 8×10^6 cm/s. Experimental results of Zanato et al [29] also shown in Fig. 5 to compare with theoretical results. It can be seen that a good agreement exists between both results.

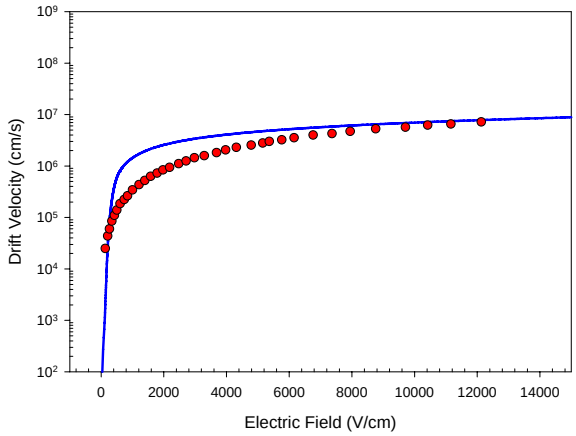

Fig. 5. Electric field dependence of drift velocity for the carrier concentration of n_e=9.0×10^{24} m^{-3} at the lattice temperature of T_o = 1.5 K. The dots show experimental results of Zanato et al [29].

When the acoustic phonon emission dominates totally the energy loss processes, the drift velocity is increasing sharply with electron temperature at T_e<2 K, which can be seen from Fig. 6. Electron heating is seen to occur for T_e>2 K. Fig. 6 also shows the most important feature of the electron temperature dependence of υ_d with T_e is the linear increase of υ_d with electron temperature. The drift velocity increase linearly with electron temperature until the electron temperature is equal to 60 K, where it makes a cusp and then decrease with electron temperature up to 130 K. At the linear region, acoustic phonon scattering process determines the electron behaviour, so the energy loss processes, and stays effective up to the end of the region, in the electron temperature range of 1.5 K<T_e<130 K. At this region, the major part of the electrons lack energy required for optical phonon emission, and the energy relaxation time is long. So, the drift velocity decreases as the electron temperature increases.

Above of this region, T_e>130 K, the polar optic phonon scattering starts to influence the electron transport and electron becomes hot and the mobility of electronic system decreases. The transition takes place from the

acoustic phonon controlled energy dissipation to the dissipation controlled by optical phonon emission. The hot phonon enhance the probability of the optical phonon emission to a certain extent, but the hot phonon reabsorption effect prevails and slow down the overall energy relaxation in region where the relaxation is controlled by the optical phonons. Due to enhanced phonon occupation number, the hot phonons support a stronger scattering of electrons. The scattering caused by the optical phonon absorption increases because of the phonon reabsorption. Thus, the scattering caused by the optical phonon emission increases due to the stimulated emission. This explains the essential reduction in the drift velocity. Above this electron temperature region, the drift velocity increases linearly with electron temperature.

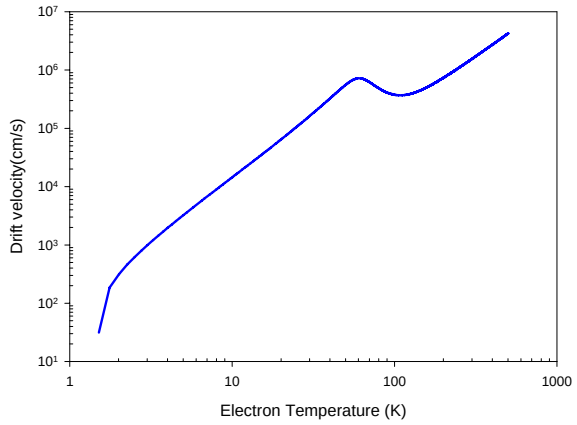

Fig. 6. Drift velocity of electrons as function of electron temperature for the electron concentration of n_e=9.0x10^{24} m^{-3} at the lattice temperature of T_o=1.5 K.

The electric field dependence of electron temperature is shown in Fig. 7. It shows that, in the very low electron temperature region, the electron temperature is almost not change and stay constant with electric field (E<100 V/cm), where the energy loss rates determined by the acoustic phonon emission due to the PZ coupling. Then, the electron heating is starting at E>200 V/cm and T_e>2 K and the electron temperature starts increasing very sharply with electric field in the range of 100<E<650 V/cm until the electron temperature reaches a value of 100 K , where is the acoustic mode phonon regime. Above this electric field range, E>650 V/cm, the electron temperature increases very slowly with electric field, where is the polar optic phonon regime. At this region, the electrons start to degenerate and hot phonons become effective. The computed results have been compared with experimental results of Zanato et al [29]. Although, the curves show similar characteristics, there is a deviation between experimental and theoretical results. The saturation values are around one order of magnitude lower than the experimental results. The reasons for the discrepancy have been given previously.

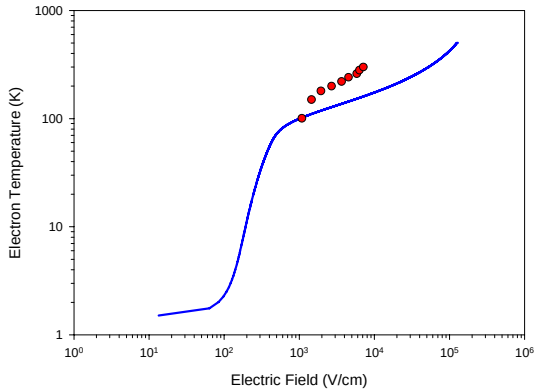

Fig. 7. Electric field dependence of electron temperature for the electron concentration of n_e=9.0x10^{24} m^{-3} at the lattice temperature of T_o=1.5 K. The dots show experimental results of Zanato et al [29].

From the figures (3-7), we can concluded that, at very low fields (E<100 V/cm) where the all of the electrons reside in the lowest subband, the drift velocity increases linearly with electric field, with a mobility of ~100 cm^2/V s. This mobility low compared to the room temperature. The low field mobility may be influenced by the electron-acoustic phonon interaction due to the PZ coupling. Above this electric field region, the mobility of electrons is the highest value of ~3000 cm^2/V s in the range of 650<E<8 kV/cm. For the electric field above 200 V/cm, the drift velocity saturates and the cool electrons become hot. The mobility of the electronic system starts to decrease at this electric field range. In fact, the more rapid increase in electron temperature with increasing electric field is responsible for the reduction in mobility and thus the drift velocity due to the enhanced electron-phonon scattering. It is possible to say that, the velocity saturation effects and repopulation of the various subband energy levels play significant roles in the velocity-field curves.

4. Conclusions

Some of the electron-phonon interaction effects through theoretical calculations of electron transport have been examined for n-type InN. Electron temperature and electron concentration dependence of energy loss rates and mobility of electrons have been investigated by using the weak perturbation based theory. The acoustic phonon scattering due to the piezoelectric coupling and the deformation potential and also the polar optic phonon emission mechanisms were taken into account for calculations of the energy loss rates and mobility of electron. The results were obtained for the electron temperatures in the range of 1.5 to 500 K at the lattice temperature of 1.5 K. It can be clearly seen that, the main energy loss processes are the acoustic phonon scattering at

low electron temperatures T_e<130 K and the optic phonon emission above this electron temperature. Also, the polar optic phonon scattering time has been obtained about 23 fs.

To test the theoretical model, the theoretical results of energy loss rates of electrons were compared with the experimental results of Zanato et al [29]. The agreement between theoretical and experimental results is good over all electron temperature. In addition, the mobility of electrons were calculated and compared with the experimental mobility measurement of Tansley et al [31] and a good agreement has been obtained, especially in the electron temperature range of T_e<130 K. Above this temperature range, the results predicts that, some other extra scattering mechanism should be included to the theory.

Acknowledgements

Authors would like to acknowledge the support received for this work from the Erciyes University Research Fund (project no: FBA-07-41).

References

[1] Y. F. Wu, B. D. Keller, S. Keller, D. Kopolnek, P. Kozuday, S. D. Denbaars, U. K. Mishra, Appl. Phys. Lett. **69**, 1438 (1996).
[2] S. N. Mohammad, A. Salvador and H. Morkoç, Proc. IEEE **83,** 1306 (1995).
[3] C. E. Martinez, N. M. Stanton, A. J. Kent, M. L. Williams, I. Harrison, H. Tang, J. B. Webb, J. A. Bardwell, Semicond. Sci. Technol. **19,** 440 (2004).
[4] K. P. Joshi, Appl. Phys. Lett., **64,** 223 (1994).
[5] H. Morkoç and S. N. Mohammad, in Wiley Enclopedia of Electrical and Electronics Engineering, edited by J. Webster. John Wiley and Sons, New York (1999).
[6] Razeghi M and Rogalski A, J. Appl. Phys. **79** 7433 (1996).
[7] I. J. Fritz, T. J. Drummond, Electron. Lett., **31,** 68 (1995).
[8] S. Nakamura et al, Jpn. J. Appl. Phys., Part 2 **38**, L1578 (1997).
[9] G. E. Bulman et al, Electron. Lett. **33,** 1556 (1997).
[10] S. Nakamura and G. Fasol, The Blue Laser Diode. Berlin: Springer (1997).
[11] T. Matsuoka, H.Okamoto, M. Nakao, H. Hirama, E. Kurimoto, Appl. Phys. Lett. **81,** 1246 (2002).
[12] V.Yu Davydov et al, Phys. Status Solidi B **229 ,** R1 (2002).
[13] J. Wu, W. Walukiewicz, K. M. Yu, J. W. Ager III, E.E. Haller, Hai Lu, W. J. Scahaff. Y. Saito and Y. Nanishi, Appl. Phys. Lett. **81,** 3967 (2002).
[14] F. Bechstedt and J. Furtmuller, J. Cryst. Growth **246** 314 (2002).
[15] B .K. Ridley, Rep. Prog. Phys. **54** 169 (1991).
[16] P. J. Price, Surf. Sci. **143** 145 (1984).
[17] E. M. Daniels, B. K. Ridley, M. Emeny, Solid-State Electron. **32** 1207 (1989).
[18] K. Lee, M. S. Shur , T. J. Drummond and H. Morkoç, J. Appl. Phys. **54** 6432 (1983).
[19] A. J. Cross, A. J. Kent, D. Lehmann, Cz. Jasiukiewicz, M. Henini, Physica B **263**, 526 (1999).
[20] S. Gokden, N. Balkan and B. K. Ridley, Semicond. Sci. Technol. **18** 206 (2003).
[21] J Shah, Solid-State Electron., **32,** 1051 (1989).
[22] R. Gupta, B. K. Ridley, Solid-State Electron. **32,** 1241 (1989).
[23] J. Shah, The Physics of The Two Dimensional Electron Gas, edited by J. T. Devreese and F. M. Peters, Plenum New York, NATO ASI Series b **157,** 183 (1987).
[24] E. M. Conwell , Solid State Physics, Supplement 9, edited by F. Seitz , D. Turnbull and H. Ehrenreich, Academic, New York (1967).
[25] K. Segeer, Semiconductor Physics: an introduction 7. ed., Springer-Verlag, Berlin (1999).
[26] S.N. Mohammad and H. Morkoç, Prog. Quant. Electron. **20** 361 (1996).
[27] V. W. L. Chin, T. L. Tansley and T. Osotchan, J. Appl. Phys. **75,** 7365 (1994).
[28] S. K. O'Learly, B. E. Foutz, M. S. Shur, L. F. Eastman, J. Mater. Sci: Mater Electron. **17,** 87 (2006).
[29] D. Zanato N. Balkan, B. K. Ridley, G. Hill, W. J. Schaff , Semicond. Sci. Technol. **19,** 1024 (2004).
[30] S. K. Pugh, D. J. Brand and R. A. Abram, Semicond. Sci. Technol. **14** 23 (1999).
[31] T. L. Tansley and C. P. Foley, Electron. Lett. **20,** 1066 (1984); T. L. Tansley, C. P. Foley, Electron lett. **20** 1087 (1984).

*Corresponding author: ari@erciyes.edu.tr